Kinetic and Theoretical Studies on the Protonation of [Ni(2-SC$_6$H$_4$N){PhP(CH$_2$CH$_2$PPh$_2$)$_2$}]$^+$: Nitrogen versus Sulfur as the Protonation Site

Athinoula L. Petrou,[†] Andreas D. Koutselos,[‡] Hilal S. Wahab,[‡,‖] William Clegg,[§] Ross W. Harrington,[§] and Richard A. Henderson*,[§]

[†]*Laboratory of Inorganic Chemistry, and* [‡]*Laboratory of Physical Chemistry, Department of Chemistry, National and Kapodistrian University of Athens, Athens 15771, Greece, and* [§]*School of Chemistry, Newcastle University, Newcastle upon Tyne, NE1 7RU, U.K.* [‖]*Permanent address: Department of Chemistry, College of Science, Al-Nahrain University, Baghdad, Iraq*

The complexes [Ni(4-Spy)(triphos)]BPh$_4$ and [Ni(2-Spy)(triphos)]BPh$_4$ {triphos = PhP(CH$_2$CH$_2$PPh$_2$)$_2$, 4-Spy = 4-pyridinethiolate, 2-Spy = 2-pyridinethiolate} have been prepared and characterized both spectroscopically and using X-ray crystallography. In both complexes the triphos is a tridentate ligand. However, [Ni(4-Spy)(triphos)]$^+$ comprises a 4-coordinate, square-planar nickel with the 4-Spy ligand bound to the nickel through the sulfur while [Ni(2-Spy)(triphos)]$^+$ contains a 5-coordinate, trigonal-bipyramidal nickel with a bidentate 2-Spy ligand bound to the nickel through both sulfur and nitrogen. The kinetics of the reactions of [Ni(4-Spy)(triphos)]$^+$ and [Ni(2-Spy)(triphos)]$^+$ with lutH$^+$ (lut = 2,6-dimethylpyridine) in MeCN have been studied using stopped-flow spectrophotometry, and the two complexes show very different reactivities. The reaction of [Ni(4-Spy)(triphos)]$^+$ with lutH$^+$ is complete within the deadtime of the stopped-flow apparatus (2 ms) and corresponds to protonation of the nitrogen. However, upon mixing [Ni(2-Spy)(triphos)]$^+$ and lutH$^+$ a reaction is observed (on the seconds time scale) to produce an equilibrium mixture. The mechanistic interpretation of the rate law has been aided by the application of MSINDO semiempirical and ADF calculations. The kinetics and calculations are consistent with the reaction between [Ni(2-Spy)(triphos)]$^+$ and lutH$^+$ involving initial protonation of the sulfur followed by dissociation of the nitrogen and subsequent transfer of the proton from sulfur to nitrogen. The factors affecting the position of protonation and the coupling of the coordination state of the 2-pyridinethiolate ligand to the site of protonation are discussed.

Introduction

Proton transfer is a common feature in many complex, multistep pathways, most notably those associated with catalysis and biology.[1] The complexity of these multistep reactions often precludes direct study of the individual component proton transfer steps. Consequently, understanding proton transfer in such systems relies on studies of simple model systems.[2] The factors which control the rates of proton transfer are, in general, relatively simple, resulting in easy prediction of the rates of proton transfer. Thus, thermodynamically favorable proton transfer to an atom (within a molecule or ion) containing a stereochemically active lone pair of electrons invariably occurs at the diffusion-controlled limit while thermodynamically unfavorable reactions of the same type are slower and occur at a rate defined by the approximate Brönsted relationship which is shown in eq 1, where k_A is the rate constant for proton transfer, K_a is the equilibrium constant for the proton dissociation reaction, and G$_A$ and α are constants.[1,3]

$$k_A = \mathrm{G_A} K_a{}^\alpha \qquad (1)$$

Exceptions to this general behavior are rare. However, it has been observed that thermodynamically favorable proton transfer reactions involving metal and carbon sites are slow.[2] It has been proposed that the reason for slow proton transfer at these sites is attributable to reorganization of the coligands (for metal sites) and rehybridization (for carbon sites).

The coordination of a molecule or ion (substrate) to a metal site can significantly affect the protonation chemistry of the substrate and, depending on the characteristics of the

*To whom correspondence should be addressed. Fax: 0191 222 6929. Phone: 0191 222 6636. E-mail: r.a.henderson@ncl.ac.uk.

(1) Eigen, M. *Angew. Chem., Int. Ed. Engl.* **1964**, *3*, 1, and refs therein.

(2) (a) Kramarz, K. W.; Norton, J. R. *Prog. Inorg. Chem.* **1994**, *42*, 1, and refs therein. (b) Kristjansdottir, S. S.; Norton, J. R. *Transition Metal Hydrides: Recent Advances in Theory and Experiment*; Dedieu, A., Ed.; VCH: New York, 1992; Chapter 9, and refs therein; (c) Henderson, R. A. *Angew. Chem., Int. Ed. Engl.* **1996**, *35*, 946, and refs therein. (d) Henderson, R. A. *Recent Advances in Hydride Chemistry*; Peruzzini, M., Poli, R., Eds.; Elsevier: Amsterdam, 2001 p 3470, and refs therein.

(3) Bell, R. P. *The Proton in Chemistry*, 2nd ed.; Chapman and Hall: London, 1973; and refs therein.
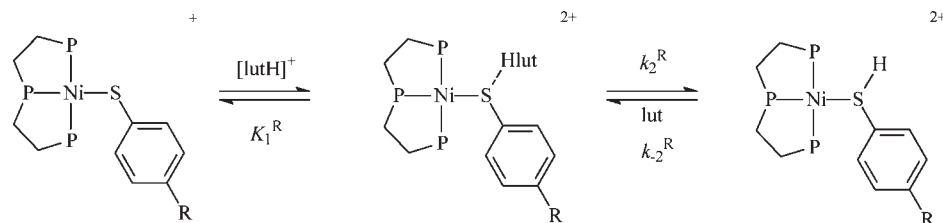
Figure 1. Mechanism for the reaction of $[Ni(SC_6H_4R\text{-}4)(triphos)]^+$ with $lutH^+$.

metal site (the metal and its coligands), can increase or decrease the acidity of the bound substrate compared to its free state. Thus, when bound to an electron-poor site (Hard Lewis acid) protonated substrates are more acidic than when free but when bound to an electron-rich site (Soft Lewis acid) protonation of the substrate can become more favorable. For the most part, this behavior is well understood only in thermodynamic terms (i.e., changes to pK_a of substrate when bound and when free). Little is known of how coordination affects the rates of proton transfer although there have been a variety of studies involving protonation of organometallic compounds where the rates of proton transfer to either the metal or the carbon-based ligand have been measured as well as any subsequent rearrangements (either inter- or intramolecular) resulting in the transfer of the proton to the thermodynamically favored product.[2]

In this paper we report studies on the protonation of 2- and 4-pyridinethiolates coordinated to the robust $\{Ni(triphos)\}^{2+}$ $\{triphos = PhP(CH_2CH_2PPh_2)_2\}$ site. In particular, for $[Ni(2\text{-}Spy)(triphos)]^+$ the site of protonation is coupled to the coordination state of the 2-pyridinethiolate ligand. The X-ray crystal structure of a salt of $[Ni(2\text{-}Spy)(triphos)]^+$ shows that both the nitrogen and sulfur are bound to nickel. Consequently, protonation by $lutH^+$ (lut = 2,6-dimethylpyridine) has to occur at the sulfur. The pK_as of free pyridinethiols indicate that protonation of sulfur by $lutH^+$ is unfavorable. Clearly, coordination facilitates protonation of the sulfur site. However, upon protonation of the sulfur, the 2-pyridinethiol chelate undergoes ring-opening, making available the lone pair of electrons on the nitrogen for protonation. Both calculations and the pK_as of the free pyridinethiols indicate that the most favored protonation site is the nitrogen. Consequently, the proton transfers from sulfur to nitrogen.

Results and Discussion

Although there is work in the literature reporting the synthesis and structural characteristics of a wide range of complexes containing pyridinethiolate ligands, particularly describing the different modes of coordination (S-bonded, N-bonded, and bidentate),[4] there are no reports on the kinetics and mechanism of protonation of this type of complex. In this paper we report the synthesis of $[Ni(2\text{-}thiopyridine)(triphos)]BPh_4$ and

$[Ni(4\text{-}thiopyridine)(triphos)]BPh_4$, their structural characterization by X-ray crystallography, together with kinetic and computational studies on the protonation of these complexes.

Protonation of thiolate ligands bound to $\{Ni(tertiary$ $phosphine)\}^{2+}$ sites has been studied earlier.[5,6] In particular, previous studies have shown that $[Ni(SC_6H_4R\text{-}4)(triphos)]^+$ $(triphos = PhP(CH_2CH_2PPh_2)_2;$ R = MeO, Me, H, Cl, or $NO_2)$ can be protonated with $lutH^+$ to form $[Ni(HSC_6H_4R\text{-}4)(triphos)]^{2+}$ in $MeCN$.[5] These are equilibrium reactions, and the kinetics exhibit a complex dependence on the concentrations of $lutH^+$ and lut, consistent with the mechanism involving two coupled equilibria as shown in Figure 1. Using stopped-flow spectrophotometry, the initial hydrogen-bonding of $lutH^+$ to the sulfur of the thiolate group can be detected, and the intramolecular proton transfer within the hydrogen-bonded adduct to transfer the proton completely to the sulfur (k_2^R) can be followed.

It is important to appreciate that there is a large difference in the basicities of the sulfur sites in thiophenols and pyridinethiolates. Protonation of the sulfur in the complexes $[Ni(SC_6H_4R\text{-}4)_2(Ph_2PCH_2CH_2PPh_2)]$ and $[Ni(SC_6H_4R\text{-}4)(triphos)]^+$ can be accomplished using $lutH^+$, and kinetic studies indicate the thiols coordinated to these Ni^{II} sites are associated with pK_a = about 14.3.[5,6] This is consistent with the calculated pK_a = 13.9 of *free* C_6H_5SH in $MeCN$, which is estimated using the literature value for the pK_a in water (pK_a = 6.6)[7] together with the relationship shown in eq 2.[8]

$$pK_a^{MeCN} = 1.313 pK_a^{H_2O} + 5.20 \qquad (2)$$

In contrast, consideration of the pK_as of *free* pyridinethiolates indicates that protonation of the sulfur in these molecules by $lutH^+$ is significantly less favorable than protonation of thiophenolate. The arguments presented here are not precise; however, they do highlight the significant thermodynamic difference in protonating a thiolate and a pyridinethiolate. The imprecision is because the pK_as of pyridinethiolates in water are calculated (not experimental), and to calculate the pK_a in $MeCN$, another approximate calculation has to be performed.

Pyridinethiols have two associated pK_as: one corresponding to protonation of the sulfur and the other corresponding to protonation of the nitrogen. The two pK_a's of the cation $HNC_5H_4SH^+$ have been reported in water[9] and, using eq 2, it

(4) Selected examples include: (a) Onaka, S.; Yaguchi, M.; Yamauchi, R.; Ozeki, T.; Ho, M.; Sunahara, T.; Sugiura, Y.; Shiotsuka, M.; Nunokawa, K.; Horibe, M.; Okazaki, K.; Iida, A.; Chiba, H.; Inoue, K.; Imai, H.; Sako, K. *J. Organomet. Chem.* **2005**, *690*, 57. (b) Zhang, L.; Zhang, H.-X.; Chen, C.-L.; Deng, L.-R.; Kang, B.-S. *Inorg. Chim. Acta* **2003**, *355*, 49. (c) Liaw, W.-F.; Lee, J.-H.; Gau, H.-B.; Chen, C.-H.; Jung, S.-J.; Hung, C.-H.; Chen, W.-Y.; Hu, C.-H.; Lee, G.-H. *J. Am. Chem. Soc.* **2002**, *124*, 1680. (d) Lopes, I.; Hillier, A. C.; Liu, S. Y.; Domingos, A.; Ascenso, J.; Galvao, A.; Sella, A.; Marques, N. *Inorg. Chem.* **2001**, *40*, 1116. (e) Deeming, A. J.; Meah, M. N.; Bates, P. A.; Hursthouse, M. B. *Inorg. Chim. Acta* **1988**, *142*, 33–37.

(5) Autissier, V.; Zarza, P. M.; Petrou, A.; Henderson, R. A.; Harrington, R. W.; Clegg, W. *Inorg. Chem.* **2004**, *43*, 3106.
(6) Autissier, V.; Clegg, W.; Harrington, R. W.; Henderson, R. A. *Inorg. Chem.* **2004**, *43*, 3098.
(7) www.cem.msu.edu/~reusch/OrgPage/acidity2.htm
(8) Kaljurand, I.; Kütt, A.; Sooväli, L.; Rodima, T.; Mäemets, V.; Leito, I.; Koppel, I. A. *J. Org. Chem.* **2005**, *70*, 1019.
(9) Albert, A.; Barlin, G. B. *J. Chem. Soc.* **1959**, 2384.

Table 1. Analytical and Spectroscopic Data for [Ni(2-Spy)(triphos)]BPh$_4$ and [Ni(4-Spy)(triphos)]BPh$_4$

complex	elemental analysis^a			^{1}H NMR spectrum	^{31}P{^{1}H} NMR spectrum
	C	H	N		
[Ni(4-Spy)(triphos)]BPh$_4$^{b}	71.8	5.68	1.37	2.6 (br, s, 8H) CH_2	53.8 (d) terminal PPh$_2$
	(71.6)	(6.10)	(1.25)	6.7−8.2 (m, 49H) aromatic CH	106.0 (t) central PPh
[Ni(2-Spy)(triphos)]BPh$_4$	73.9	5.62	1.37	2.6, 2.7, 2.1 (br, s, 8H) CH_2	51.4 (d) terminal PPh$_2$
	(74.0)	(5.57)	(1.36)	6.2−7.3 (m, 49H) aromatic CH	115.8 (t) central PPh

^{a} Calculated values in parentheses. ^{b} Isolated with 2MeOH and 0.5 thf in crystals.
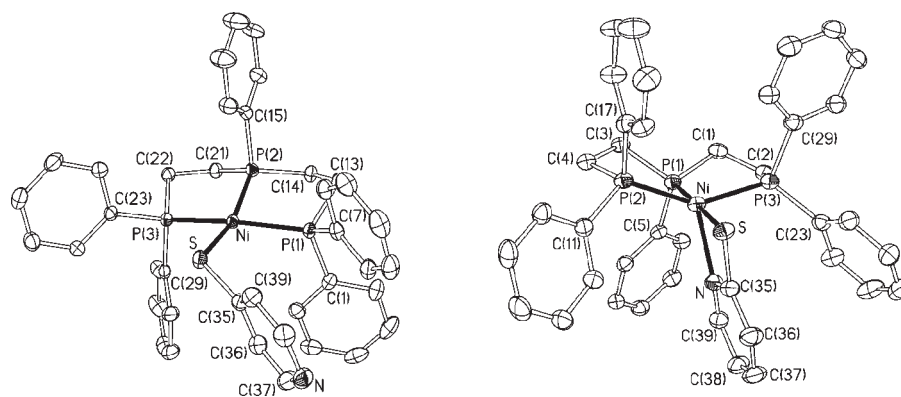
Figure 2. Structures of [Ni(4-Spy)(triphos)]$^+$ (left) and [Ni(2-Spy)(triphos)]$^+$ (right) with 50% probability displacement ellipsoids and selected atom labels. H atoms are omitted for clarity.

can be calculated that, for the 2-pyridinethiol cation in MeCN, pK_a^S = 3.9 and pK_a^N = 17.9 and for 4-pyridinethiol:cation pK_a^S = 8.1 and pK_a^N = 20.8. However, we cannot calculate the equilibrium constants for protonation (by lutH$^+$) of the sulfur and nitrogen sites in the pyridinethiols using these pK_as, since we require the pK_as of the neutral species HNC$_5$H$_4$S and NC$_5$H$_4$SH which are unavailable. However, (simply based on the charge) it would be expected that the pK_as of pyridinethiol would be higher than the corresponding pK_as of HNC$_5$H$_4$SH$^+$ (i.e., both the nitrogen and the sulfur in the neutral species would be more basic than in the cation). These arguments indicate that in free 2-pyridinethiol (i) the sulfur in pyridinethiols is significantly less basic than in thiophenols and is not capable of being protonated by lutH$^+$ (pK_a = 14.13 in MeCN)^{8,10} but that (ii) the nitrogen is much more basic than the sulfur.

X-ray Crystal Structures of [Ni(2-Spy)(triphos)]BPh$_4$ and [Ni(4-Spy)(triphos)]BPh$_4$·2MeOH·0.5thf. The lithium salts of 2-pyridinethiolate and 4-pyridinethiolate both react with [NiCl(triphos)]BPh$_4$ to produce (after workup and recrystallization from CH$_2$Cl$_2$/Et$_2$O) red crystalline solids. Analysis and spectroscopic data of both compounds (Table 1) show that they have the formulation [Ni(pyridinethiolate)(triphos)]BPh$_4$ (pyridinethiolate: 2-pyridinethiolate = 2-Spy; 4-pyridinethiolate = 4-Spy). However, X-ray crystallography shows that their structures are different. The structures of the cations [Ni(4-Spy)(triphos)]$^+$ and [Ni(2-Spy)(triphos)]$^+$ are shown in Figure 2. The crystal data and structure refinement parameters for both complexes are presented in Table 2.

The structure of [Ni(4-Spy)(triphos)]$^+$ is similar to that of [Ni(SC$_6$H$_5$)(triphos)]$^+$ reported earlier.^{15} The Ni is

(10) Izutsu, K. *Acid-Base Dissociation Constants in Dipolar Aprotic Solvents*; Blackwells Scientific: Oxford, U.K., 1990.

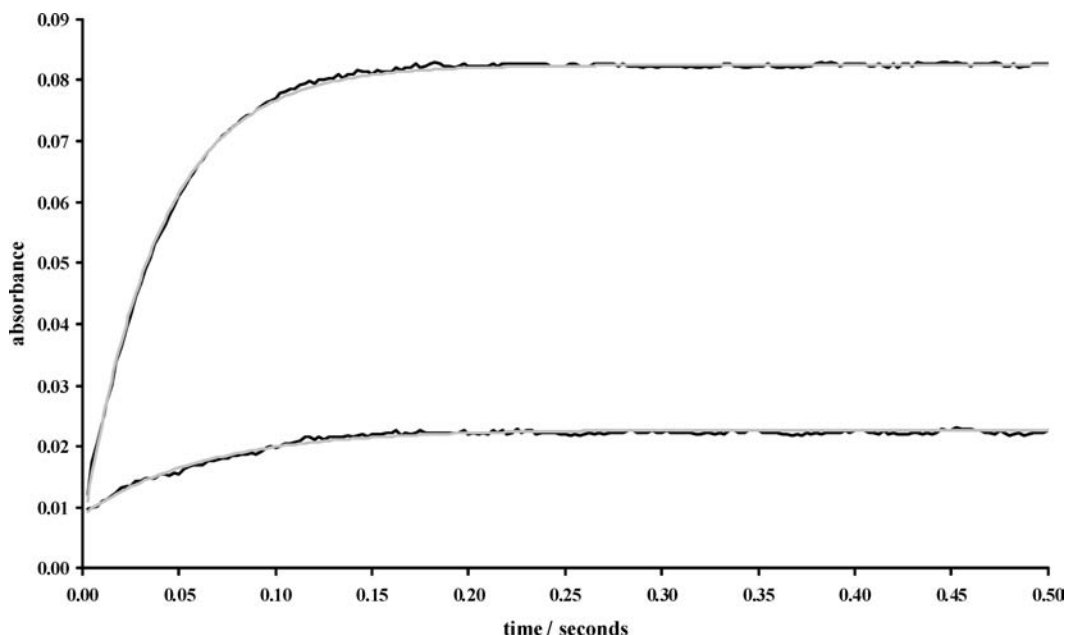**Table 2.** Crystal Data and Structure Refinement Parameters for [Ni(2-Spy)(triphos)]BPh$_4$ and Solvated [Ni(4-Spy)(triphos)]BPh$_4$

	[Ni(2-Spy)(triphos)]BPh$_4$	[Ni(4-Spy)(triphos)]BPh$_4$ 2CH$_3$OH·0.5C$_4$H$_8$O
chemical formula	C$_{63}$H$_{57}$BNNiP$_3$S	C$_{67}$H$_{69}$BNNiO$_{2.5}$P$_3$S
molecular weight	1022.59	1122.7
crystal system	triclinic	triclinic
space group	P$\bar{1}$	P$\bar{1}$
T, K	120	160
a, Å	12.6807(15)	11.6661(6)
b, Å	13.1347(15)	14.3526(7)
c, Å	17.164(2)	20.1381(10)
α, deg	105.0751(9)	73.159(2)
β, deg	97.1106(9)	73.332(2)
γ, deg	97.4014(10)	67.844(2)
V, Å^3	2700.2(5)	2928.4(3)
Z	2	2
λ, Å	0.6727	0.71073
μ, mm^{-1}	0.527	0.495
reflections measured	22208	24838
unique data, R$_{int}$	10862, 0.0419	13054, 0.0331
refined params	631	712
R (F, F^2 > 2σ)	0.0451	0.0460
R$_W$ (F^2, all data)	0.1069	0.1334
GoF (F^2)	1.012	1.036
max, min el dens (e Å^{-3})	0.59, −0.34	0.95, −0.56

4-coordinate with the geometry best described as square planar {angles: P(2)−Ni−P(3) = 85.04(2)°, P(2)−Ni−P(1) = 84.99(2)°, P(3)−Ni−P(1) = 159.79(3)°, P(3)−Ni−S = 91.22(3)°, P(1)−Ni−S = 103.44(3)°, P(2)−Ni−S = 162.02(3)°}. The pyridinethiolate is coordinated through the sulfur atom to Ni {Ni−S = 2.1830(7) Å}, with the angle Ni−S−C(35) = 115.54(8)°. The sulfur is *trans* to the central phosphorus of the triphos ligand. The Ni−P bond lengths are unremarkable {Ni−P(1) = 2.2096(7) Å, Ni−P(2) = 2.1405(7) Å, Ni−P(3) = 2.2029(7) Å}.

Figure 3. Typical stopped-flow absorbance-time curves for the reaction of [Ni(2-Spy)(triphos)]$^+$ (0.1 mmol dm^{-3}) with lutH$^+$ in the presence of lut in MeCN at 25.0 °C (λ = 385 nm). The upper curve was recorded with [lutH$^+$] = 2.5 mmol dm^{-3} and [lut] = 2.0 mmol dm^{-3} and the lower curve with [lutH$^+$] = 2.5 mmol dm^{-3} and [lut] = 10.0 mmol dm^{-3}. The gray curves are the exponential fits to each curve. For the upper curve the fit is defined by the equation A_t = 0.0825 − 0.0715e$^{-25.7t}$, and for the lower curve the fit is defined by the equation A_t = 0.0226 − 0.0133e$^{-15.2t}$.

In contrast, the structure of [Ni(2-Spy)(triphos)]$^+$ contains a 5-coordinate Ni. The structure is best described as a distorted trigonal bipyramid with the trigonal plane comprising the two terminal phosphorus atoms of the triphos ligand {Ni−P(2) = 2.1637(9) Å, Ni−P(3) = 2.1996(9) Å} and the nitrogen of the 2-Spy ligand {Ni−N = 2.164(2) Å}. The two axial positions are occupied by the central phosphorus of the triphos ligand {Ni−P(1) = 2.1310(8) Å} and the sulfur {Ni−S = 2.2644(8) Å}. The principal origin of the distortion is the small bite angle associated with the 2-Spy ligand {S−Ni−N = 70.81(6)°}. Other bond angles that define the coordination geometry of the Ni atom in [Ni(2-Spy)(triphos)]$^+$ are as follows: P(1)−Ni−P(2) = 87.08(3)°, P(1)−Ni−P(3) = 87.08(3)°, P(2)−Ni−P(3) = 146.34(3)°; P(1)−Ni−S = 178.98(4)°, P(2)−Ni−S = 92.08(3)°, P(3)−Ni−S = 93.93(3)°; P(1)−Ni−N = 109.12(7)°, P(2)−Ni−N = 119.08(7)°, P(3)−Ni−S = 94.11(7)°.

Reaction between [Ni(4-Spy)(triphos)]$^+$ and lutH$^+$. When monitored using a stopped-flow spectrophotometer (at several wavelengths in the range λ = 350−450 nm), mixing [Ni(4-Spy)(triphos)]$^+$ (0.1 mmol dm^{-3}) and lutH$^+$ is associated with a very small absorbance decrease complete within the dead-time of the stopped-flow apparatus (2 ms). We have studied this reaction with [lutH$^+$] = 0.1−5.0 mmol dm^{-3}, [lut] = 0.2 mmol dm^{-3}, and monitored over short and protracted times (5 ms−5 min). Under all conditions, even using equimolar amounts of [Ni(4-Spy)(triphos)]$^+$ and lutH$^+$ and in the presence of a large excess of lut, no reaction other than the small absorbance decrease complete within the dead-time is observed. The structure of [Ni(4-Spy)(triphos)]$^+$ is very similar to that of [Ni(SC$_6$H$_5$)(triphos)]$^+$ which is readily protonated at the sulfur by lutH$^+$. Consequently, it seems unlikely that the reason the sulfur atom in [Ni(4-Spy)-(triphos)]$^+$ is not protonated by lutH$^+$ is attributable to

steric factors. Rather, the inability of lutH$^+$ to protonate the sulfur of [Ni(4-Spy)(triphos)]$^+$ is consistent with the sulfur in coordinated 4-pyridinethiolate being insufficiently basic to be protonated by lutH$^+$. The rapid reaction associated with the observed small absorbance change is most probably due to protonation of the nitrogen (remote from the metal) by lutH$^+$. It would be anticipated that protonation of the nitrogen to form [Ni(4-SpyH)(triphos)]$^{2+}$ would decrease the basicity of the coordinated sulfur even further, making this site even less favorable to protonation by lutH$^+$.

Reaction between [Ni(2-Spy)(triphos)]$^+$ and lutH$^+$. When studied using stopped-flow spectrophotometry, the reaction between [Ni(2-Spy)(triphos)]$^+$ and lutH$^+$ in the presence of lut shows absorbance-time curves with a significant amplitude over the seconds time scale. Typical absorbance-time curves (measured at λ = 385 nm) are shown in Figure 3. Furthermore, the magnitude of the absorbance-time curves are characteristic of an equilibrium protonation reaction as indicated in eq 3. Thus, under all conditions, the initial absorbance of the absorbance-time curves corresponds to that of [Ni(2-Spy)(triphos)]$^+$ at the concentration used ([Ni] = 0.5 mmol dm^{-3}), but the final absorbance varies. Consistent with the equilibrium reaction shown in eq 3, the spectrophotometric changes increase in magnitude as the concentration of lutH$^+$ is increased (at a constant concentration of lut), and decrease as the concentration of lut increases (at a constant concentration of lutH$^+$). This behavior is markedly different to that observed in the irreversible reaction of [Ni(2-Spy)(triphos)]$^+$ with anhydrous HCl ([HCl] = 2−10 mmol dm^{-3}) in MeCN, to form [NiCl(triphos)]$^+$ and 2-pyridinethiol. In limited studies using [HCl] = 2−10 mmol dm^{-3}, the reaction with the stronger acid HCl (pK_a in MeCN = 8.9)[10] is associated with a single exponential absorbance decrease, with both the initial and the final
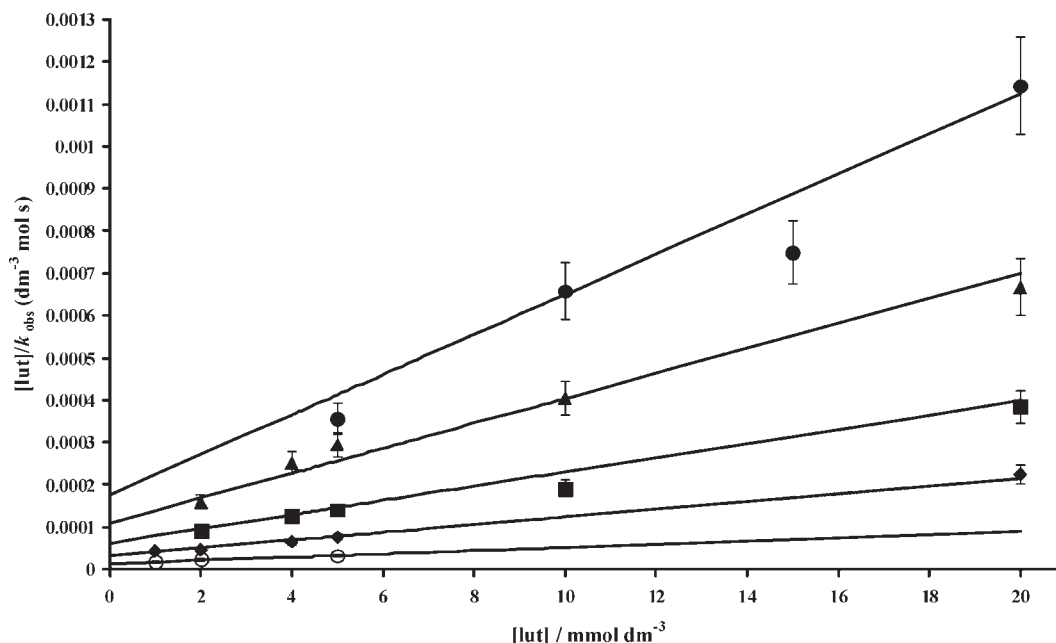
Figure 4. Kinetic data for the reaction between $[Ni(2\text{-Spy})(triphos)]^+$ (0.1 mmol dm^{-3}) and $lutH^+$ in the presence of lut (solvent = MeCN, λ = 385 nm, T = 25.0 °C). Data points correspond to: $[lutH^+]/[lut]$ = 0.25, $[lut]$ = 5−20 mmol dm^{-3} (●); $[lutH^+]/[lut]$ = 0.50, $[lut]$ = 2−20 mmol dm^{-3} (▲); $[lutH^+]/[lut]$ = 1.0, $[lut]$ = 2−20 mmol dm^{-3} (■); $[lutH^+]/[lut]$ = 2.0, $[lut]$ = 1−20 mmol dm^{-3} (♦); $[lutH^+]/[lut]$ = 5.0, $[lut]$ = 1−5 mmol dm^{-3} (○). The straight line fits are those defined by eq 5. Additional data is presented in Supporting Information which also is a good fit to eq 5. See text for details of the analysis of these data.

absorbances unaffected by the concentration of acid.

$$[Ni(2\text{-Spy})(triphos)]^+ + lutH^+$$

$$\overset{K_0}{\rightleftharpoons} [Ni(2\text{-SpyH})(triphos)]^{2+} + lut \qquad (3)$$

Kinetics of the Protonation Reaction. The spectrophotometric changes observed in the reactions between $[Ni(2\text{-}Spy)(triphos)]^+$ and $lutH^+$ in the presence of lut indicates this is an equilibrium reaction. If the reaction were a simple single-step equilibrium then the rate law for the reaction would be that described by eq 4, where the rate of the reaction would increase as the concentration of either $lutH^+$ or lut is increased.[11] However, analysis of the kinetic results for the reaction between $[Ni(2\text{-Spy})\text{-}(triphos)]^+$ and an excess of $lutH^+$ and lut shows that the rate of the reaction *increases* as the concentration of $lutH^+$ increases but *decreases* as the concentration of lut increases.

$$\frac{-d[Ni(2\text{-Spy})(triphos)^+]}{dt}$$

$$= \{k_{forward}[lutH^+] + k_{back}[lut]\}[Ni(2\text{-Spy})(triphos)^+]$$
$$(4)$$

When $[lutH^+]/[lut]$ is kept constant, plots of $[lut]/k_{obs}$ versus $[lut]$ are a straight line. Varying $[lutH^+]/[lut]$ produces a series of straight lines and as $[lutH^+]/[lut]$ increases the straight lines have decreasing gradient and intercept, as shown in Figure 4. A least-squares analysis of these data yields the rate law shown in eq 5. It is important to note that the data in the graphical analysis of Figure 4 show significant scatter making precise

(11) Espenson, J. H. *Chemical Kinetics and Reaction Mechanism*; McGraw-Hill: New York, 1981.

analysis difficult.

$$\frac{-d[Ni(2\text{-Spy})(triphos)^+]}{dt} =$$

$$\frac{\{(1.38 \pm 0.20 \times 10^4)[lutH^+] + (2.23 \pm 0.20 \times 10^3)[lut]\}[Ni(2\text{-Spy})(triphos)^+]}{\{1 + (2.69 \pm 0.20 \times 10^2)[lut]\}}$$

$$(5)$$

While these kinetics and the spectrophotometric changes indicate that $[Ni(2\text{-Spy})(triphos)]^+$ is protonated by $lutH^+$, we will defer until later identification of the protonation site of $[Ni(2\text{-Spy})(triphos)]^+$.

Mechanism of Reaction between $[Ni(2\text{-Spy})(triphos)]^+$ and $lutH^+$ in the Presence of lut. We will now discuss the details of the protonation chemistry of $[Ni(2\text{-Spy})\text{-}(triphos)]^+$ as revealed by the kinetic analysis, the pK_as, and calculations.

Sites of Protonation. The key issue concerns where $[Ni(2\text{-Spy})(triphos)]^+$ binds protons. We have been unable to isolate the protonated complex because of the equilibrium nature of this protonation reaction. Attempts to isolate the product by using a stronger acid (HCl), and hence drive the equilibrium shown in eq 3 to the right-hand side, resulted in the loss of 2-HSpy and formation of $[NiCl(triphos)]^+$ (vide supra). Similar behavior has been observed in the reaction of $[Ni(SC_6H_5)(triphos)]^+$ with HCl.[15] In principle, there are four possibilities as shown in Figure 5: at sulfur or nitrogen in the closed or open structures. Alternative structures with the nitrogen coordinated and the sulfur free seem unreasonable because in $[Ni(4\text{-Spy})(triphos)]^+$, where either nitrogen or sulfur could bind, coordination occurs at the sulfur. Furthermore, our calculation studies show no indication that an N-bonded (S-open) structure of $[Ni(2\text{-Spy})(triphos)]^+$ represents an energy minimum.
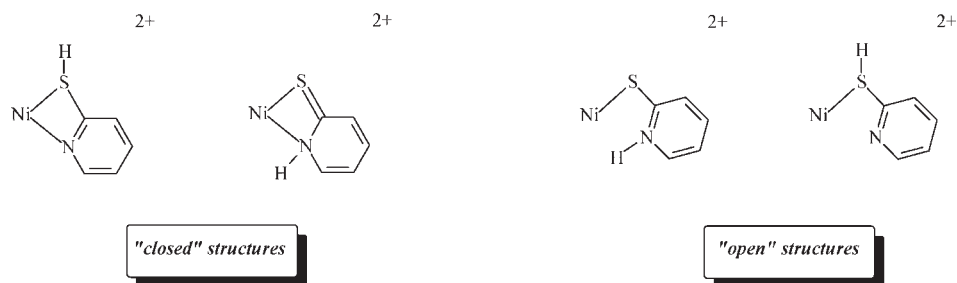
Figure 5. Possible structures of protonated [Ni(2-Spy)(triphos)]$^+$ (triphos ligand omitted for clarity).

To explore the protonation chemistry of [Ni(2-Spy)-(triphos)]$^+$ we have applied a variety of theoretical methods (MSINDO, ADF, and CPMD). Initially, we studied the structure of [Ni(2-Spy)(triphos)]$^+$ in the gas phase and explored the sites of protonation, especially sulfur and nitrogen, through MSINDO and Amsterdam Density Functional (ADF) calculations. As detailed below, both methods indicate that the initial site of protonation of [Ni(2-Spy)(triphos)]$^+$ is the sulfur but the energy-favored product is the "open" structure with the nitrogen protonated. However, MSINDO and ADF calculations do not give a consistent answer about the relative energies of these two protonated species. Parenthetically, we should mention that the Car–Parrinello Molecular Dynamics (CPMD) method (which was used for molecular dynamics (MD) simulation of H transfer in a simplified molecular structure, with phenyl groups replaced by H), produces a different result, with the "closed" structure where sulfur is protonated appearing to be more stable than the "open" structure where nitrogen is protonated. However, this result should be considered to be less reliable than those with MSINDO or ADF because of the drastic modifications applied to the molecular structure.

Using the unaltered "closed" structure of [Ni(2-Spy)-(triphos)]$^+$ established by X-ray crystallography, MSINDO semiempirical calculations indicate that the bound sulfur is more basic than the bound nitrogen, and consequently the sulfur site would protonate preferentially (i.e., there is a lone pair of electrons available on sulfur but none on the bound nitrogen). However, in the "open" structure where the 2-pyridinethiolate is bound to nickel only by the sulfur, nitrogen was found to be more basic than the coordinated sulfur. Energy calculations have shown that the thermodynamically favored protonated species contains the "open" 2-pyridinethiolate ligand with a protonated nitrogen.

To further substantiate the results of the MSINDO semiempirical calculations, we have applied a density functional computational method, ADF, at the level of TZP basis set, to the calculation of the protonated structures of [Ni(2-Spy)(triphos)]$^+$. The ADF method converged only when the starting configuration was approximated by an "open" complex (i.e., nitrogen not coordinated). All attempts to obtain a converged structure with the nitrogen both protonated and coordinated to nickel failed, indicating that such a structure may be impossible to obtain numerically and therefore to exist. Using the ADF method, the "open" structure with the nitrogen protonated is found to be about 13.2 kcal mol^{-1} more stable than the "closed" structure with sulfur

protonated. The MSINDO method predicts the same relative stability property of the two open structures but with a quite smaller energy difference, of about 0.19 kcal mol^{-1}.

The numerical difference in these energy calculations originates from the approximation of the two approaches. ADF is a density functional method that is based on approximate functional integrals about the correlation and exchange energy, while MSINDO is based on the neglect of complex interaction matrix elements of Molecular Orbital theory. The different nature of the two approaches makes comparison of the results difficult. Further, since the calculations refer to gas-phase structures it is not justifiable to relate the energies to the kinetic studies that were performed in MeCN as the solvent. However, the experimentally observed rapidity and reversibility of the reaction between [Ni(2-Spy)(triphos)]$^+$ and [lutH]$^+$ favors the MSINDO result, since the ADF result indicates $K_4 \sim 10^{-10}$ at 25 °C.

Mechanism of Protonation. For the reaction of [Ni(2-Spy)(triphos)]$^+$ with lutH$^+$ in the presence of lut, we suggest that the experimentally observed rate law {eq 5} together with the calculations presented above, are consistent with the mechanism shown in Figure 6. This mechanism consists of two coupled equilibrium reactions in which the first step is protonation of [Ni(2-Spy)-(triphos)]$^+$ at the sulfur to form an intermediate, which then undergoes a unimolecular equilibrium reaction to form the "open" structure with nitrogen protonated. Consideration of this mechanism, assuming that the sulfur-protonated species is a steady state intermediate, shows that the associated rate law is that shown in eq 6. Comparison of eqs 5 and 6 gives the values: $k_3 = (1.38 \pm 0.20) \times 10^4$ dm^3 mol^{-1} s^{-1}; $k_{-3}/k_4 = (2.69 \pm 0.20) \times 10^2$ dm^3 mol^{-1}, and $k_{-4} = 8.29 \pm 2$ s^{-1}. However, as we will see when we consider the second step in this equilibrium, it seems unlikely that k_4 and k_{-4} are true elementary rate constants. Rather, the transfer of the proton from sulfur to nitrogen most likely involves several steps.

$$\frac{-\mathrm{d}[\text{Ni(2-Spy)}(\text{triphos})^+]}{\mathrm{d}t}$$

$$= \frac{\{(k_3[\text{lutH}^+] + (k_{-3}k_{-4}/k_4)[\text{lut}]\}[\text{Ni(2-Spy)}(\text{triphos})^+]}{1 + (k_{-3}/k_4)[\text{lut}]}$$

$$(6)$$

Previous work[5] on the protonation of other, related, Ni-thiolate complexes [Ni(SC$_6$H$_4$R-4)(triphos)]$^+$ indicated a mechanism involving the rapid equilibrium
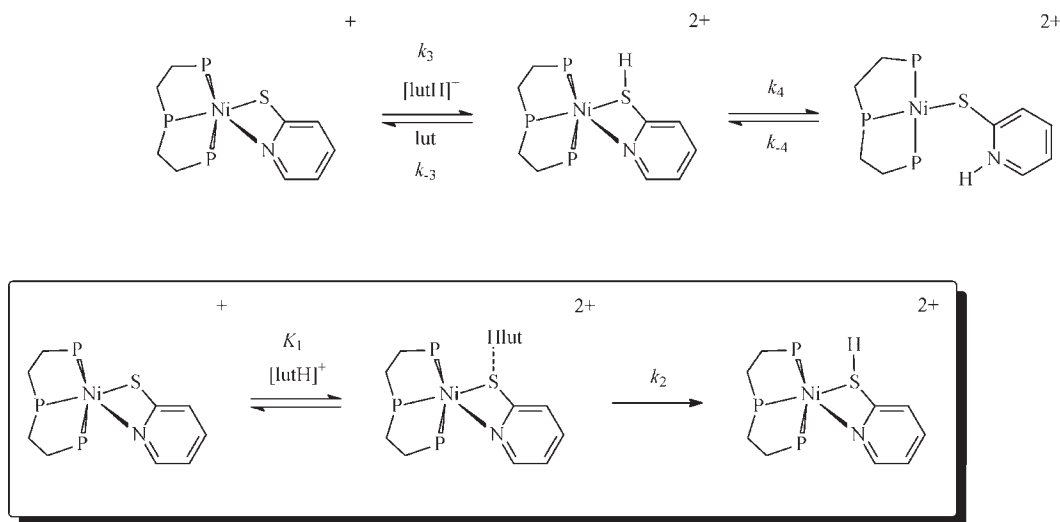
Figure 6. Top line shows the mechanism for the protonation of [Ni(2-Spy)(triphos)]$^+$ by lutH$^+$ in MeCN. The pathway presented in the box shows the proposed detail for transfer of the proton involving initial hydrogen bonding of lutH$^+$ to the complex (K_1) prior to intramolecular proton transfer (k_2). Such hydrogen bonding has been detected previously in the reactions of lutH$^+$ with [Ni(SC$_6$H$_4$R-4)(triphos)]$^+$ (see Figure 1). However, in the reaction with [Ni(2-Spy)(triphos)]$^+$ the value of K_1 is small.

formation of a hydrogen-bonded adduct between the complex and lutH$^+$ (Figure 1). It seems likely that a similar hydrogen-bonded adduct is formed between [Ni(2-Spy)(triphos)]$^+$ and lutH$^+$ and that in reality the k_3 step involves the initial formation of a hydrogen-bonded adduct (K_1) prior to the complete transfer of the proton to the sulfur (k_2) as shown in the inset of Figure 6. For such a sequence of reactions, k_3[lutH$^+$] = $K_1 k_2$[lutH$^+$]/(1 + K_1[lutH$^+$]). However, in the reaction with [Ni(2-Spy)(triphos)]$^+$ the concentration of the hydrogen bonded adduct does not accumulate and so K_1[lutH$^+$] < 1 and k_3[lutH$^+$] = $K_1 k_2$[lutH$^+$]. Thus, the kinetics and mechanism presented here for the reaction between [Ni(2-Spy)(triphos)]$^+$ and lutH$^+$ are consistent with the kinetics and mechanism proposed earlier for the reactions of [Ni(SC$_6$H$_4$R-4)(triphos)]$^+$ with lutH$^+$.

The overall equilibrium constant for the mechanism shown in Figure 6 (K_0) is related to the elementary rate constants by the expression $K_0 = k_3 k_4/k_{-3}k_{-4}$. Using the values of the rate constants determined from the kinetic analysis, we can calculate $K_0 = 6.19 \pm 0.9$.

We can independently estimate the overall equilibrium constant (K_0) for the reaction from spectrophotometric analysis of the effects that the concentrations of lutH$^+$ and lut have on the absorbance changes in the reaction with [Ni(2-Spy)(triphos)]$^+$ (Figure 3). By considering the equilibrium reaction between [Ni(2-Spy)(triphos)]$^+$ and lutH$^+$ to form [Ni(2-SpyH)(triphos)]$^{2+}$ and lut, and using Beer's Law, it can be shown that the variation of the final absorbance of the stopped-flow trace, A_{eq} (i.e., absorbance of the equilibrium mixture of [Ni(2-Spy)(triphos)]$^+$ and [Ni(2-SpyH)(triphos)]$^{2+}$), is related to the ratio [lutH$^+$]/[lut] as shown in eq 7, provided that neither lutH$^+$ nor lut absorb at the wavelength being used (λ = 385 nm). In eq 7, [Ni(2-Spy)(triphos)]$_i$ = 0.5 mmol dm^{-3}, ε_{Ni} = 38.0 dm^3 mol^{-1} cm^{-1} (extinction coefficient [Ni(2-Spy)-(triphos)]$^+$, λ = 385 nm), and ε_{NiH} = 228.5 dm^3 mol^{-1} cm^{-1} (extinction coefficient [Ni(2-SpyH)(triphos)]$^{2+}$, λ = 385 nm). It is important to emphasize that the derivation of eq 7 is consistent with only a single proton being transferred to [Ni(2-Spy)(triphos)]$^+$.

$$\frac{1}{A_f - \varepsilon_{Ni}[\text{Ni(2-Spy)(triphos)}^+]_i}$$
$$= \frac{1}{K_0(\varepsilon_{NiH} - \varepsilon_{Ni})[\text{Ni(2-Spy)(triphos)}^+]_i[\text{lutH}^+]/[\text{lut}]}$$
$$+ \frac{1}{(\varepsilon_{NiH} - \varepsilon_{Ni})[\text{Ni(2-Spy)(triphos)}^+]_i} \quad (7)$$

The plot of $1/(A_f - \varepsilon_{Ni}[\text{Ni(2-Spy)(triphos)}^+]_i)$ versus [lut]/[lutH$^+$] is shown in Figure 7. To measure absorbance differences more accurately, we have used a larger concentration of [Ni(2-Spy)(triphos)]$^+$ = 0.5 mmol dm^{-3} in the studies to determine the equilibrium constant than in the kinetic studies ([Ni(2-Spy)(triphos)]$^+$ = 0.1 mmol dm^{-3}). Although the plot is a straight line, it is clear that there is a high degree of scatter on the data and, in particular, that there appears to be a systematic deviation from the line at low [lut]/[lutH$^+$]. These features result in large uncertainties to the measured gradient and intercept of the line. Since the gradient = $1/\{K_0(\varepsilon_{NiH} - \varepsilon_{Ni})[\text{Ni(2-Spy)(triphos)}^+]_i\}$ and the intercept = $1/\{(\varepsilon_{NiH} - \varepsilon_{Ni})[\text{Ni-(2-Spy)(triphos)}^+]_i\}$, K_0 = intercept/gradient = 3.0 ± 1.0.

Clearly, the agreement between the value of K_0 determined from the kinetics and that determined from the spectrophotometric analysis is not very good. We believe the reason for this poor agreement is that at the wavelength used (λ = 385 nm) there is a small contribution to the absorbance from lutH$^+$ and/or lut (both of which are present in a large excess over the concentration of complex). This would affect the spectrophotometric analysis, in particular, increasing the gradient of the plot at low [lut]/[lutH$^+$] and leading to a lower calculated value of K_0 when determined spectrophotometrically.

We will now consider each of the steps in the mechanism shown in Figure 6 (the protonation and the rearrangement) in turn. This mechanism indicates that, upon coordination as a bidentate ligand, the sulfur in 2-pyridinethiolate of the "closed" structure of [Ni(2-Spy)(triphos)]$^+$ is sufficiently
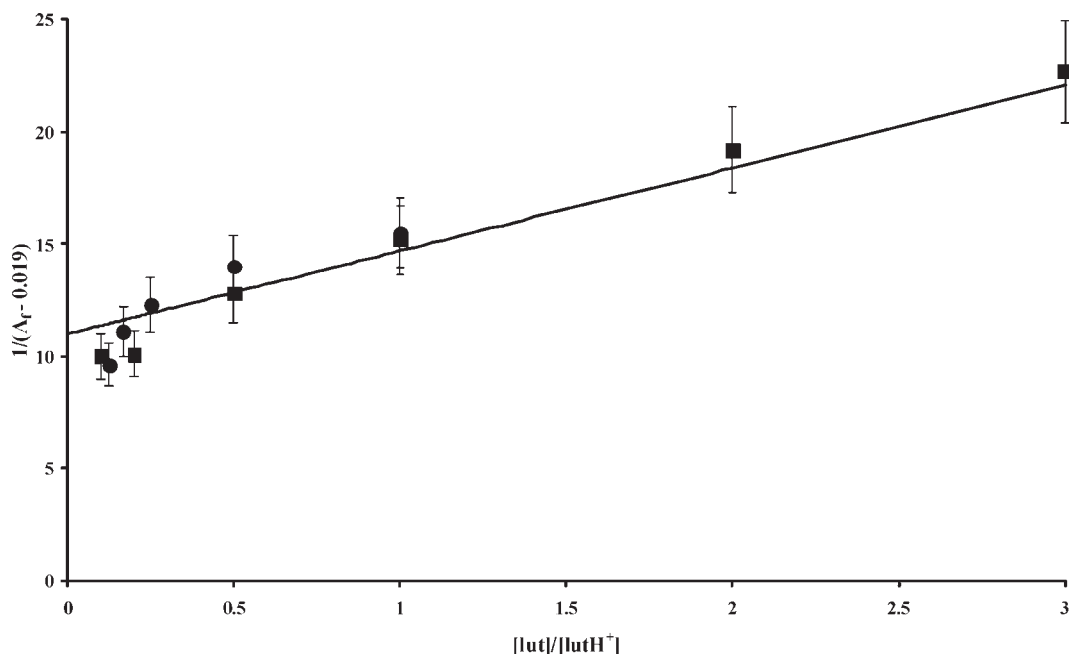
Figure 7. Analysis of the spectrophotometric data to determine the overall equilibrium constant (K_0) for the reaction between [Ni(2-Spy)(triphos)]$^+$ and lutH$^+$ in the presence of lut (solvent = MeCN, λ = 385 nm, T = 25.0 °C). Plot of $1/(A_f - \varepsilon_{Ni}[Ni(2\text{-Spy})(triphos)^+]_i)$ versus [lut]/[lutH$^+$] {A_f = final absorbance of absorbance-time curve (see Figure 3) measured in the presence of known concentrations of lutH$^+$ and lut; ε_{Ni} = molar extinction coefficient of [Ni(2-Spy)(triphos)]$^+$; [Ni(2-Spy)(triphos)$^+$] = 0.5 mmol dm^{-3}}. Data points correspond to: [lutH$^+$] = 0.5–10 mmol dm^{-3}, [lut] = 1.0 mmol dm^{-3} (●); [lutH$^+$] = 10 mmol dm^{-3}, [lut] = 1.0–30 mmol dm^{-3} (■). The straight line fit is that defined by eq 7 and by the parameters presented in the text.

basic to be protonated by lutH$^+$ (p$K_a{}^{lutH}$ = 14.13 in MeCN).[8] The observation that [Ni(4-Spy)(triphos)]$^+$ is not protonated at sulfur by lutH$^+$ indicates that coordination of only the sulfur of a pyridinethiolate to the {Ni(triphos)}$^{2+}$ site is insufficient to make the sulfur basic enough to be protonated by lutH$^+$. The increased basicity of the sulfur in the 2-pyridinethiolate ligand must be a consequence of the bidentate ligation of 2-pyridinethiolate resulting in redistribution of the electron density toward sulfur.

The kinetic analysis presented above allows us to calculate the rate constant for protonation of the sulfur in [Ni(2-Spy)(triphos)]$^+$ by lutH$^+$ (k_3 = 1.38 ± 0.20 × 10^4 dm^3 mol^{-1} s^{-1}). Previous studies have shown that the rates of proton transfer from lutH$^+$ to thiolate sulfurs bound to Ni^{II} sites in [Ni(SC$_6$H$_5$)(triphos)]$^+$ and [Ni-(SC$_6$H$_5$)$_2$(Ph$_2$PCH$_2$CH$_2$PPh$_2$)] fall in the range $k \sim$ 20–200 dm^3 mol^{-1} s^{-1}. The rate of proton transfer to [Ni(2-Spy)(triphos)]$^+$ is appreciably faster than that measured for [Ni(SC$_6$H$_4$R)(triphos)]$^+$ and [Ni(SC$_6$H$_4$R)$_2$-(dppe)] with lutH$^+$. It is not entirely clear why this should be so, but it could be that the juxtaposition of the nitrogen and sulfur atoms in [Ni(2Spy)(triphos)]$^+$ results in an enhanced rate of proton transfer to the sulfur through anchimeric assistance,[12] in which the approach of the acid toward the sulfur is aided by the proximal electronegative nitrogen.

The experimental (kinetics) results give little information about the nature of the second step shown in Figure 6, except that it occurs at a rate independent of the concentrations of lutH$^+$ or lut. Processes consistent with such kinetics could be (i) a geometrical change at the nickel

with no bond cleavage, (ii) cleavage of a Ni−P bond, or (iii) cleavage of the Ni−N bond. We conclude that the second step involves Ni−N bond cleavage for the following reasons. First, we have used calculations to explore whether geometrical changes occur to [Ni(2-SpyH)-(triphos)]$^{2+}$, and have found no evidence of such structural reorganization. Second, there is no evidence that the phosphine dissociates from the complex. Thus, ^{31}P{^{1}H} NMR spectra of mixtures comprising [Ni(2-Spy)-(triphos)]$^+$ and lutH$^+$ show patterns characteristic of the triphos ligand where two terminal phosphorus and one central phosphorus are all coordinated to the nickel.

The MSINDO and ADF calculations described above indicate that the thermodynamically favored product of the reaction between [Ni(2-Spy)(triphos)]$^+$ and lutH$^+$ contains the "open" 2-pyridinethiolate ligand with the nitrogen protonated. We therefore propose that, after initial protonation of the sulfur to form the "closed" [Ni(2-SpyH)(triphos)]$^{2+}$, that the nitrogen dissociates from the nickel, thus freeing the lone-pair of electrons on nitrogen to be protonated. In line with the results of the MSINDO and ADF calculations, we suggest that the pendant nitrogen in the "open" 2-pyridinethiol ligand is more basic than the coordinated sulfur, and so the proton transfers from sulfur to nitrogen. The possible pathways for the proton transfer between sulfur and nitrogen are summarized in Figure 8. Because the kinetics of the second step in the mechanism (Figure 6) occur at a rate independent of the concentrations of lutH$^+$ or lut, proton transfer must either be intramolecular (i.e., direct transfer from sulfur to nitrogen), in which, after dissociation of the nitrogen from the "closed" [Ni(2-SpyH)(triphos)]$^{2+}$, rotation about the C−S bond occurs and the proton hops from sulfur to the more basic nitrogen, or intermolecular involving rapid movement of the proton mediated by

(12) Calveresi, M.; Rinaldi, S.; Arcelli, A.; Garavelli, M. *J. Org. Chem.* **2008**, *73*, 2066, and refs therein.
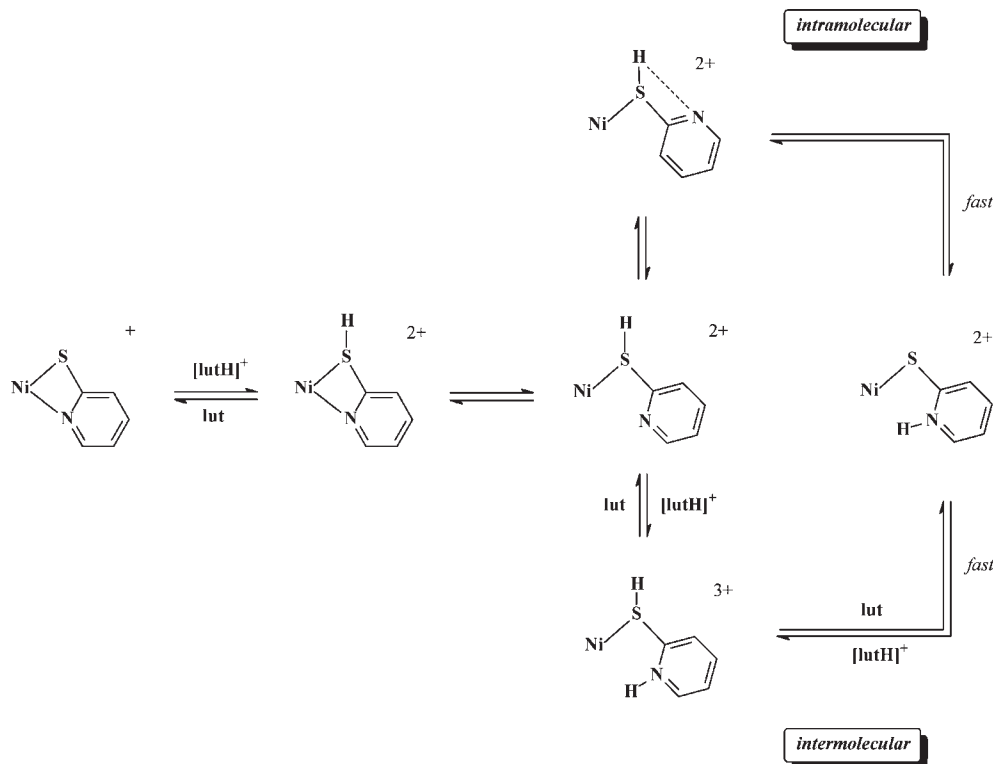
Figure 8. Possible intramolecular and intermolecular pathways for the transfer of proton from sulfur to nitrogen in the reaction of [Ni(2-Spy)(triphos)]$^+$ with lutH$^+$ in MeCN. Another intermolecular pathway (not shown) is possible in which deprotonation of the sulfur precedes protonation of the pendant nitrogen. For this pathway to be viable, the protonation of the pendant nitrogen would have to be faster than the rate at which the nitrogen coordinates to the nickel.

lutH$^+$ and lut, after the slow dissociation of the Ni−N bond.

Despite the apparent reasonableness of the intramolecular processes, it is not supported by calculations. Previous theoretical studies on free pyridones indicated that the intramolecular pathway was of very high energy.[13] In addition, direct transfer of a proton between nitrogen and sulfur has been studied using the CPMD method for a simplified complex where phenyl groups are replaced by hydrogen for computational convergence and efficiency. The calculations have identified an apparent saddle point with the proton lying between the nitrogen and sulfur atoms (at a line positioned in between sulfur and nitrogen and inclined at 30° toward nickel). However, the energy barrier for this pathway is calculated to be greater than 45 kcal mol^{-1} and so appears not to be feasible.

In the absence of support for an intramolecular pathway, we suggest that the prototropic shift is accomplished by an acid−base-catalyzed pathway similar to that suggested earlier for pyridones. In solutions containing an excess of lutH$^+$ and lut, the "transfer" of the proton is accomplished rapidly, after the dissociation of the nitrogen from nickel. Such an acid−base-catalyzed transfer is shown in the bottom line of Figure 8. After dissociation of the Ni−N bond, rapid protonation of the nitrogen ensues

because of the availability of the lone pair of electrons. On the basis of purely charge considerations, this protonation would be expected to decrease the basicity of the sulfur, resulting in proton dissociation from this site.

Isotope Experiments. We have studied the effect on the kinetics of using lutD$^+$ in the reaction with [Ni(2-Spy)(triphos)]$^+$ in the presence of lut. The results are presented in Figure 9. This figure shows plots of [lut]/k_{obs} versus [lut] at constant [lutH$^+$]/[lut] = 2. Clearly, because of the multistep nature of the reaction, the interpretation of the effect is not simple.[14] Considering the mechanism shown in Figure 6, it seems most reasonable to propose that both k_3 and k_{-3} would be associated with primary isotope effects. Although the second stage must also involve proton movement we suggest that the rate of this stage is limited by dissociation of the Ni−N bond and so has no, or very minor, deuterium isotope effects. Several lines are presented in Figure 9. In addition to the line defined by eq 6, there are also lines defined by the same rate law but which show the influence of different isotope effects for k_3 and k_{-3}, ranging from the extremes where $k_3{}^H/k_3{}^D = 2$, $k_{-3}{}^H/k_{-3}{}^D = 1$ to $k_3{}^H/k_3{}^D = 1$, $k_{-3}{}^H/k_{-3}{}^D = 2$ and where k_3 and k_{-3} have the same isotope effect, $k_3{}^H/k_3{}^D = 2$, $k_{-3}{}^H/k_{-3}{}^D = 2$. Two features of these plots are worth comment. First, it is evident that, depending on the relative isotope effects associated with k_3 and k_{-3}, the overall effect can appear to be a normal or an inverse

(13) (a) Lowry, T. H.; Richardson, K. S. *Mechanisms and Theory in Organic Chemistry*; Harper and Row: New York, 1976; p 426; (b) Swain, C. G.; Brown, J. F., Jr. *J. Am. Chem. Soc.* **1952**, *74*, 2534. (c) Swain, C. G.; Brown, J. F., Jr. *J. Am. Chem. Soc.* **1952**, *74*, 2538. (d) Rony, P. R. *J. Am. Chem. Soc.* **1968**, *90*, 2824. (e) Rony, P. R. *J. Am. Chem. Soc.* **1969**, *91*, 6090. (f) Rony, P. R.; Neff, R. O. *J. Am. Chem. Soc.* **1973**, *95*, 2896. (g) Li, Y.; Guo, Y.; Li, B. *Huaxue Yanjiu.* **2006**, *17*, 71 (chinese, abstract only).

(14) For discussions of normal and inverse primary isotope effects see, for example: (a) Parkin, G. *Acc. Chem. Res.* **2009**, *42*, 315, and refs therein. (b) Truhlar, D. C.; Garrett, B. C. *Isotope Effects in Chemistry and Biology*; Kohen, A., Limbach, H.-H., Eds.; Taylor and Francis: New York, 2006; reference, Chapters 11 and 12.
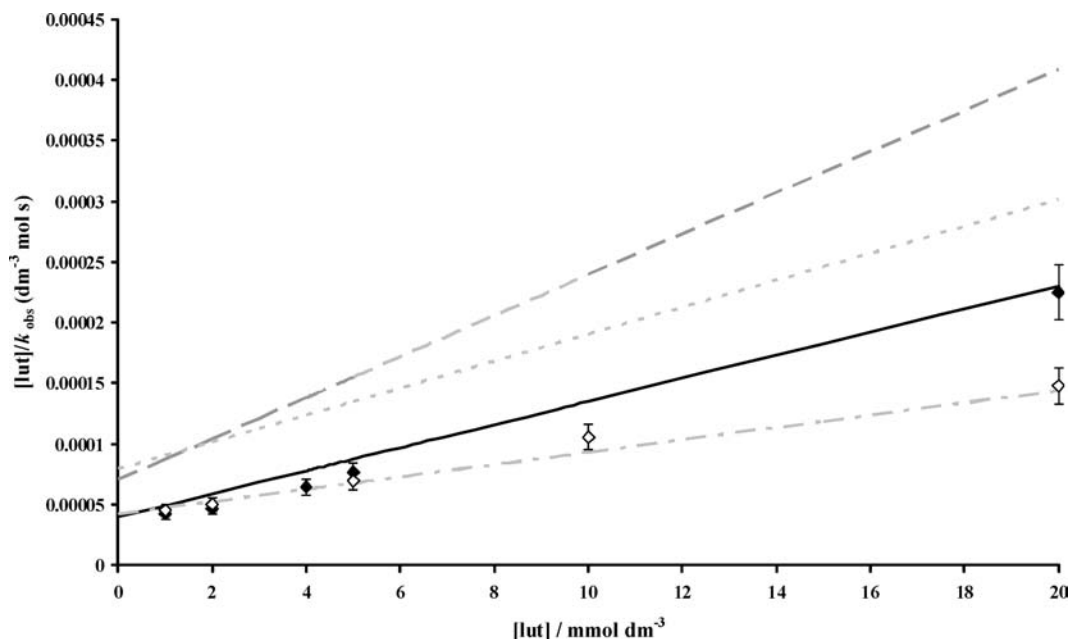
Figure 9. Plot of $[\text{lut}]/k_{\text{obs}}$ versus $[\text{lut}]$ for the reaction between $[\text{Ni(2-Spy)(triphos)}]^+$ and lutD^+ in the presence of lut in MeCN at 25.0 °C, illustrating how various deuterium isotope effects associated with k_3 and k_{-3} affect the kinetics. In all plots $[\text{lutH}^+]/[\text{lut}] = 2.0$. The dark, solid line and the data points shown as solid diamonds ($\blacklozenge$) correspond to that for the reaction with lutH^+ as defined by eq 6. The gray lines correspond to simulations of observed dependences, using eq 6 when $k_3^H/k_3^D = 2.0$, $k_{-3}^H/k_{-3}^D = 1.1$ (gray long-dashed line); $k_3^H/k_3^D = 2.0$, $k_{-3}^H/k_{-3}^D = 2.0$ (gray short-dashed line); and $k_3^H/k_3^D = 1.1$, $k_{-3}^H/k_{-3}^D = 2.0$ (gray dashed-dotted line). For the reaction between $[\text{Ni(2-Spy)(triphos)}]^+$ and lutD^+ in the presence of lut the data points are shown as open diamonds ($\diamondsuit$).

isotope effect, and, second, the isotope effect due to k_3 is primarily reflected in the intercept and the isotope effect due to k_{-3} is mostly reflected in the slope.

The quality of the experimental data and the complexity of the kinetic analysis, together with the way that subtle changes to the values of k_3 and k_{-3} (because of isotopic substitution) affect the plots (as shown in Figure 9) mean that it is difficult to accurately measure the isotope effects. However, the data indicate that the isotope effect for k_{-3} is larger than k_3, and we can estimate $k_3^H/k_3^D = 1.1$, $k_{-3}^H/k_{-3}^D = 2.0$. Thus, the apparent inverse isotope effect is actually attributable to the k_{-3} step having a larger primary isotope effect than k_3.

Conclusions

In considering the protonation chemistry of complexes where the ligands can undergo intramolecular changes, the question of how protons move between various basic sites on the ligand needs to be addressed. This paper describes a combined study using calculation methods and experimental kinetic studies to understand the protonation chemistry of coordinated pyridinethiolates. The pyridinethiolate is just one example of a type of ligand in which there is more than one potential protonation site and more than one type of coordination mode.

Our studies show, not unexpectedly, that, even in complexes, protonation of the nitrogen is preferred thermodynamically over protonation of sulfur. However, when the nitrogen is coordinated to the metal (as in $[\text{Ni(2-Spy)-(triphos)}]^+$), the lone pair of electrons is unavailable. Consequently, protonation at the sulfur is enforced. Coordination to the $\{\text{Ni(triphos)}\}^{2+}$ site must make the sulfur sufficiently basic to be protonated by lutH^+, and it seems likely that, at least in part, the basicity of the coordinated sulfur is a

consequence of the coordination of the nitrogen. Protonation of the sulfur results in breaking of the Ni−N bond, and when free, the proton effectively transfers to the nitrogen (now the most basic site). However, in the presence of lut the whole reaction is reversible, with deprotonation of the pendant N−H group allowing recoordination of the nitrogen to the Ni site. Thus, there is a mutual control of ligation mode and protonation site of the coordinated pyridinethiolate.

Experimental Section

All preparations and manipulations were performed under an atmosphere of dinitrogen using Schlenk and syringe techniques as appropriate. All solvents were dried and distilled from the appropriate drying agent and were used immediately after their preparation. 2-Pyridinethiol, 4-pyridinethiol, and lut were purchased from Aldrich and were used as received. $[\text{NiCl(triphos)}]\text{BPh}_4$,[15] $[\text{lutH}]\text{BPh}_4$, and $[\text{lutD}]\text{BPh}_4$[16] were prepared by methods reported in the literature. ^1H NMR spectroscopy showed that $[\text{lutD}]\text{BPh}_4$ was at least 90% deuterium-labeled.

Preparation of $[\text{Ni(2-Spy)(triphos)}]\text{BPh}_4$ and $[\text{Ni(4-Spy)-(triphos)}]\text{BPh}_4$. Both complexes were prepared by the same method. Only the preparation of $[\text{Ni(2-Spy)(triphos)}]\text{BPh}_4$ will be described here.

A slurry of $[\text{NiCl(triphos)}]\text{BPh}_4$ (2.0 g, 1.96 mmol) in tetrahydrofuran (thf, ca. 20 mL) was stirred rapidly, and Na[2-Spy] (0.30 g, 2.2 mmol) was added. The solution rapidly turned from yellow to dark red. After stirring at room temperature for 2 h, the solution was concentrated in vacuo. An excess of methanol (3−4 volumes) was added and, upon standing, red crystals of the product were formed slowly. The crystals were removed by filtration, washed with methanol and diethyl ether, then dried

(15) Clegg, W.; Henderson, R. A. *Inorg. Chem.* **2002**, *41*, 1128.
(16) Grönberg, K. L. C.; Henderson, R. A.; Oglieve, K. E. *J. Chem. Soc., Dalton Trans.* **1998**, 3093.

in vacuo. The crude solid was recrystallized by dissolving the solid in dichloromethane, filtering to remove any insoluble material, then layering methanol (2−3 volumes) on the solution. After 2−3 days the dark red crystals were removed by filtration, washed with a small amount of cold methanol, then diethyl ether, and dried in vacuo. Yield = 0.52 g, 26%. To grow crystals of [Ni(4-Spy)(triphos)]BPh$_4$ suitable for X-ray crystallography the recrystallization was performed by dissolving in the minimum of thf, then layering with methanol.

X-ray Crystallography. Data were collected on a Bruker APEX2 diffractometer with synchrotron radiation (at Daresbury Laboratory SRS station 9.8) for the 2-Spy complex and with a Bruker SMART 1K diffractometer with MoKα radiation for the 4-Spy complex. Semiempirical absorption corrections were applied, based on repeated and symmetry-equivalent data. The structures were solved by direct methods and refined on all unique F^2 data, with anisotropic displacement parameters for non-H atoms, and isotropic displacement parameters for riding H atoms. In the case of the 4-Spy complex, solvent molecules were identified and refined, without H atoms as these could not be unambiguously positioned; the asymmetric unit contains two methanol molecules and half of a thf molecule, which is disordered over an inversion center such that it is not possible to distinguish C and O atoms (all were refined as C, with restraints on geometry and displacement parameters). Programs were standard Bruker control and integration software, SHELXTL, and local programs.

Kinetic Studies. All kinetic studies were conducted using an Applied Photophysics SX 18MV stopped-flow spectrophotometer, constructed to handle oxygen-sensitive solutions. The temperature was maintained at 25.0 ± 0.1 °C using a Grant LT D6G recirculating thermostatted tank. All solutions were prepared under an atmosphere of dinitrogen and were transferred by gastight, all-glass syringes into the stopped-flow spectrophotometer. The solutions of the Ni complexes and those comprising mixtures of lut and [lutH]BPh$_4$ (or [lutD]BPh$_4$) solutions were prepared from freshly made stock solutions and were used within 2 h.

All kinetics were studied under pseudo first order conditions in acetonitrile. The concentration of the prepared stock solutions of the nickel complexes was always 0.2 mmol dm^{-3}, so that when studied by stopped-flow spectrophotometry the concentration was 0.1 mmol dm^{-3}. The concentrations of lut and lutH$^+$ ranged from 1 to 30 mmol dm^{-3} and from 2 to 12 mmol dm^{-3}, respectively. The ratio [lutH$^+$]/[lut] ranged from 0.25 to 5. The reaction of the [Ni(S-2py)(triphos)]$^+$ with lutH$^+$ in the presence of lut was studied at λ = 385 nm. At this wavelength there is an increase in absorbance, as shown in Figure 3. Presumably, this increase in absorbance at this wavelength is a consequence of the reaction involving the chelate ring-opening of the 2-thiopyridine ligand with a necessary decrease in coordination number of the Ni. Interestingly, the reaction of [Ni(SC$_6$H$_4$R-4)(triphos)]$^+$ with [lutH]$^+$, at λ = 350 nm, is associated with an absorbance decrease, but this reaction only involves protonation of the sulfur and no gross structural changes at Ni.[5]

The dependences of k_{obs} on the concentrations of lut and lutH$^+$ were determined graphically as described in the text. The values of k_{obs} presented are the average of at least three duplicate experiments where the values of k_{obs} all agree within 10%, and this is reflected in the error bars presented in Figures 4, 7, and 9.

Calculation Methods. MSINDO (Version 3.2.1)[17−20] is a method for quantum molecular dynamics at the level of the Intermediate Neglect of Differential Overlap (INDO) semiempirical self-consistent field (SCF) Molecular Orbital method with MD calculations based on the lower Born−Oppenheimer

energy surface. Here, the energy was calculated with the structure optimized alongside, with energy convergence criterion below 10^{-9} hartree. In one case MD was performed at constant temperature using Nosé−Hoover−Chain (NHC) thermostat. All complex structure calculations were based on the structure of [Ni(2-Spy)(triphos)]$^+$ as determined by X-ray crystallography. Conformation and intramolecular H-transfer barrier calculations were based on minimal pyridinethiolate deformations.

ADF (Version 2004.01) is the Amsterdam Density Functional program[21] based on the density functional theory, (DFT), and implemented through the use of Slater type basis orbitals. We have employed the TZP (core double-ζ, valence triple-ζ with polarization) basis set, which is one of the most extended sets of the method, because it can provide efficiently convergent results. Technically, the method is based on Vosko−Wilk−Nusair (VWN) functional and the Perdew−Zunger self-interaction correction (SIC) which is implemented self-consistently through the use of the Krieger−Li−Iafrate approximation to the optimized effective potential.[22] Difficulties in the convergence of the whole optimized structures did not allow us to proceed beyond the Local Density Approximation level of calculation.

CPMD (Version 3.11.1)[23] is a program for Car−Parrinello molecular dynamics method, at the level of DFT through the use of BLYP[24,25] functional that includes a gradient correction contribution as proposed by Becke[24] and the correlation energy term of Lee et al.[25] The core−valence interactions were described by semilocal norm-conserving Martins−Troullier pseudopotentials,[26] and the plane-wave expansion of the electronic states included waves up to 100 Ry.[27] During the calculations, first, the energy was minimized for an initial structure, then the structure was optimized and MD simulation was followed with attention that the electron temperature would not increase. Only a simplified structure of the complex was amenable to calculations. The full structure did not converge.

Supporting Information Available: X-ray crystallographic files for [Ni(2-Spy)(triphos)]BPh$_4$ and [Ni(4-Spy)(triphos)]BPh$_4$· 2MeOH·0.5thf. Listings of tables containing the observed rate constants for the reactions between [Ni(2-Spy)(triphos)]$^+$ and lutH$^+$ in the presence of lut. Details of the theoretical calculations and video films showing calculated movement of proton between the saddle point and nitrogen or sulfur. This material is available free of charge via the Internet at http://pubs.acs.org.

(17) Ahlswede, B.; Jug, K. *J. Comput. Chem.* **1999,** *20,* 563.
(18) Ahlswede, B.; Jug, K. *J. Comput. Chem.* **1999,** *20,* 572.
(19) Bredow, T.; Geudtner, G.; Jug, K. *J. Comput. Chem.* **2001,** *22,* 861.
(20) Steveson, M.; Bredow, T.; Gerson, A. *Phys. Chem. Chem. Phys.* **2002,** *4,* 358.
(21) *ADF, Amsterdam Density Functional software*; Scientific Computing and Modelling N. V., Faculty of Sciences, Theoretical Chemistry, Vrije Universiteit: De Boelelaan 1083, 1081 HV Amsterdam, The Netherlands (www.scm.com).
(22) (a) Patchkovskii, S.; Ziegler, T. *J. Chem. Phys.* **2001,** *115,* 26. (b) Patchkovskii, S.; Ziegler, T. *J. Chem. Phys.* **2002,** *116,* 7806. (c) Patchkovskii, S.; Ziegler, T. *J. Phys. Chem. A* **2002,** *106,* 1088.
(23) *CPMD code*, Version 3.11.1; Copyright IBM Corp. 1990−2006, Copyright MPI fur Festkorperforschung, Stuttgart, Germany, 1997−2001.
(24) Becke, A. D. *Phys. Rev. A.* **1988,** *38,* 3098.
(25) Lee, C. T.; Yang, W.; Parr, R. G. *Phys. Rev. B.* **1988,** *37,* 785.
(26) Troullier, N.; Martins, J. L. *Phys. Rev. B.* **1991,** *43,* 1993.
(27) Laasonen, K.; Pasquarello, A.; Car, R.; Lee, C.; Vanderbilt, D. *Phys. Rev. B.* **1993,** *47,* 10142.